# Phase Noise Mitigation in Channel Parameter Estimation for TDM MIMO Channel Sounding

Taparugssanagorn, Attaphongse; Yin, Xuefeng; Ylitalo, Juha; Fleury, Bernard Henri

*Published in:*
Conference Record of the Forty-First Asilomar Conference on Signals, Systems and Computers, 2007. ACSSC 2007

*DOI (link to publication from Publisher):*
10.1109/ACSSC.2007.4487295

*Publication date:*
2007

*Document Version*
Publisher's PDF, also known as Version of record



*Citation for published version (APA):*
Taparugssanagorn, A., Yin, X., Ylitalo, J., & Fleury, B. H. (2007). Phase Noise Mitigation in Channel Parameter Estimation for TDM MIMO Channel Sounding. In *Conference Record of the Forty-First Asilomar Conference on Signals, Systems and Computers, 2007. ACSSC 2007* (pp. 656-660). Electrical Engineering/Electronics, Computer, Communications and Information Technology Association. https://doi.org/10.1109/ACSSC.2007.4487295

# Phase Noise Mitigation in Channel Parameter Estimation for TDM MIMO Channel Sounding

Attaphongse Taparugssanagorn*, Xuefeng Yin‡, Juha Ylitalo†, and Bernard H. Fleury‡§

*Centre for Wireless Communications, University of Oulu, Finland, email: pong@ee.oulu.fi
†Elektrobit, Oulu, Finland
‡Department of Electronic Systems, Section Navigation and Communications, Aalborg University, Aalborg, Denmark
§Forschungszentrum Telekommunikation Wien (ftw.), Vienna, Austria

***Abstract*— Multi-input multi-output (MIMO) radio channel sounders commonly employ time-division multiplexing (TDM) techniques to switch between the elements of the transmit and receive antenna arrays. However, phase noise of the local oscillators in the transmitter and the receiver of a TDM MIMO channel sounder can significantly affect the accuracy of estimates of relevant channel parameters, such as the channel capacity and the parameters of propagation paths. In this paper we derive a new SAGE algorithm for path parameter estimation that compensates for the effect of phase noise. Monte Carlo simulations show that the new algorithm always outperforms the traditional SAGE algorithm [2], [3] and that it is able to practically mitigate this effect, provided the phase noise variance is below a certain threshold. The general conclusion is that the new SAGE algorithm is able to compensate for the effect of phase noise in practical channel sounding equipments, provided the used sounding sequences are sufficiently short. Further investigations are needed to quantitatively assess the relationship between the maximum duration of the used sounding sequences and the short-term statistics of phase noise for this compensation to be effective.**

## I. Introduction

The high-resolution SAGE algorithm [1], which provides an iterative approximation of the Maximum Likelihood (ML) estimator has been initially applied to channel parameter estimation in MIMO channel sounding [2], [3]. Most advanced MIMO radio channel sounders employ the time division multiplexing (TDM) technique for data acquisition since it saves hardware cost and reduces the effort of system calibration procedure. Nonetheless, recently published theoretical investigations show that phase noise in the local oscillators at the transmitter and the receiver of channel sounders can cause significant errors in the estimation of key channel parameters, like the channel capacity [4], [5] and the parameters characterizing multipath components [6]. In these works, phase noise is assumed to be a white process and a random walk process respectively. These assumptions however deviates to a more of less extent from the real features of phase noise, as for instance observed from measurements. For the estimation of the above parameters, the short-term behaviour of phase noise is critical, i.e. the behaviour of phase noise within one measurement cycle when all sub-channels of the MIMO channel are sounded once. Experimental evidence shows that within this time scale consecutive phase noise samples are correlated, due to the finite bandwidth of the filters in the phase locked loop oscillators in the TX and RX of the sounding equipment. This correlation strongly affects the performance of channel parameter estimates [7].

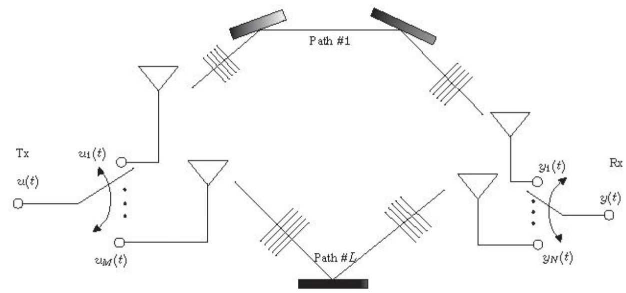


Fig. 1. TDM MIMO channel sounding.

In this paper, we propose a new SAGE algorithm, which is derived for a signal model incorporating the effect of phase noise and therefore inherently accounts and compensates for this effect. We compare the behaviour and performance of the new scheme with the traditional SAGE algorithm [2],[3] in synthetic narrowband one-path and two-path scenarios in the presence of phase noise.

The rest of the paper is organized as follows. Section II presents the signal model for TDM channel sounding in the presence of phase noise. A SAGE algorithm is derived based on this model to estimate the DOD, the DOA and the Doppler frequency in Section II. Section III analyzes the performance of the new scheme in the above scenarios. Finally, Section IV concludes the paper.

## II. Signal Model for TDM channel sounding

The TDM switched MIMO channel sounder is equipped with switches at both the transmitter (Tx) and receiver (Rx) as illustrated in Fig. 1. The electromagnetic waves propagate along $L$ different paths from the $M$ transmit antennas to the $N$ receive antennas.

We consider narrowband transmission, implying that the product of the signal bandwidth times the channel delay spread is much smaller than one. Following [2] the sounding signal $u(t)$ consists of a periodically repeated burst signal $u_s(t)$ of

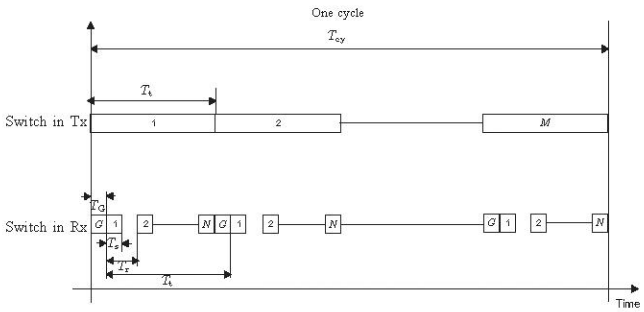


Fig. 2. Timing structure of TDM sounding.

duration $T_s$, i.e.

$$u(t) = \sum_{l=0}^{\infty} u_s(t - lT_s). \tag{1}$$

The burst signal is of the form

$$u_s(t) = \sum_{k=0}^{K-1} a_k p(t - kT_p), \tag{2}$$

with $[a_0, \ldots, a_{K-1}]$ denoting one period of a pseudo-noise (PN) sequence of length $K$ and $p(t)$ standing for the shaping pulse, whose duration $T_p$ is related to $T_s$ according to $T_s = KT_p$. As depicted in Fig. 2 the signal $u(t)$ is applied by means of Switch 1 successively at the input of each element of Array 1 during a period $T_t$.

At the Rx the switch is activated as depicted in the same figure. The outputs of the elements of Array 2 are successively scanned, each during a period $T_s$. During one measurement cycle each receive antenna element is scanned once, while each transmit antenna element is active once. The interval between two successive scans is $T_r = 2T_s$. The guard interval $T_g$ accounts for the switching time as well as any related transient effects [8].

Referring to Fig. 2 the beginning of the interval when the antenna element pair $(n, m)$ is switched in the $i$th cycle is

$$\begin{aligned} t_{i,n,m} =& (i - \frac{I+1}{2})T_{cy} + (n - \frac{N+1}{2})T_r \\ &+ (m - \frac{M+1}{2})T_t \end{aligned} \tag{3}$$

with $T_{cy}$ denoting one cycle duration and $I$ being the total number of cycles. The time reference $t = 0$ is selected to be the center of gravity of the total observation range corresponding to the $I$ measurement cycles.

Following [8], in the case without phase noise the output signal of the receive array can be written as the $NM \times I$ matrix

$$\mathbf{Y} = \sum_{\ell=1}^{L} \mathbf{s}(\boldsymbol{\theta}_\ell) + \mathbf{w}. \tag{4}$$

In (4) the vector $\boldsymbol{\theta}_\ell = [\boldsymbol{\Omega}_{1,\ell}, \boldsymbol{\Omega}_{2,\ell}, \tau_\ell, \nu_\ell, \alpha_\ell]$ embodies the parameters characterizing the $\ell^{\text{th}}$ path. More specifically, $\boldsymbol{\Omega}_{1,\ell}$, $\boldsymbol{\Omega}_{2,\ell}$, $\tau_\ell$, $\nu_\ell$, and $\alpha_\ell$ denote respectively the DOD, the DOA, the propagation delay, the Doppler frequency, and the complex weight of the $\ell^{\text{th}}$ path. A direction is characterized by a unit vector $\boldsymbol{\Omega}$ anchored at a given reference point. The vector $\boldsymbol{\Omega}$ is uniquely determined by its spherical coordinates $(\phi, \theta) \in [-\pi, \pi) \times [0, \pi]$ according to the relation

$$\boldsymbol{\Omega} = [\cos(\phi)\sin(\theta), \sin(\phi)\sin(\theta), \cos(\theta)].$$

The coordinates $\phi$ and $\theta$ are respectively the azimuth and the co-elevation of $\boldsymbol{\Omega}$. The responses of the transmit and receive arrays to a wave impinging from direction $\boldsymbol{\Omega}$ are denoted by $c_1(\boldsymbol{\Omega}) = [c_{1,1}(\boldsymbol{\Omega}), \ldots, c_{1,M}(\boldsymbol{\Omega})]$ and $c_2(\boldsymbol{\Omega}) = [c_{2,1}(\boldsymbol{\Omega}), \ldots, c_{2,N}(\boldsymbol{\Omega})]$, respectively. The signal component $\mathbf{s}(\boldsymbol{\theta}_\ell) \in \mathbb{C}^{NM \times I}$ in (4) is given by

$$\mathbf{s}(\boldsymbol{\theta}_\ell) = [\mathbf{s}(t_1; \boldsymbol{\theta}_\ell), \ldots, \mathbf{s}(t_i; \boldsymbol{\theta}_\ell), \ldots, \mathbf{s}(t_I; \boldsymbol{\theta}_\ell)], \tag{5}$$

where

$$\begin{aligned} \mathbf{s}(t_i; \boldsymbol{\theta}_\ell) = & [s(t_{i,1,1}; \boldsymbol{\theta}_\ell), \ldots, s(t_{i,N,1}; \boldsymbol{\theta}_\ell), \ldots, \\ & s(t_{i,1,M}; \boldsymbol{\theta}_\ell), \ldots, s(t_{i,N,M}; \boldsymbol{\theta}_\ell)]^{\mathrm{T}}, \end{aligned} \tag{6}$$

with

$$\begin{aligned} & s(t_{i,n,m}; \boldsymbol{\theta}_\ell) = \\ & \qquad \alpha_\ell \exp\{j2\pi\nu_\ell t_{i,n,m}\} c_{2,n}(\boldsymbol{\Omega}_{2,\ell}) c_{1,m}(\boldsymbol{\Omega}_{1,\ell})^{\mathrm{T}}. \end{aligned} \tag{7}$$

Finally, $\mathbf{w}$ in (4) denotes matrix-valued complex white Gaussian noise with component variance $\sigma_w^2$.

Due to phase noise caused by the local oscillators in the Tx and the Rx of the MIMO channel sounder each signal term in (4) is modulated by a phasor with argument depending on phase noise sampled at the corresponding signaling time. Let us define the phasor matrix $\mathbf{exp}(j\boldsymbol{\varphi})$, where $\mathbf{exp}$ is the element-wise exponential, $\boldsymbol{\varphi} = [\boldsymbol{\varphi}(t_1), \ldots, \boldsymbol{\varphi}(t_i), \ldots, \boldsymbol{\varphi}(t_I)]$ and

$$\begin{aligned} \boldsymbol{\varphi}(t_i) \;=\; & [\varphi(t_{i,1,1}), \ldots, \varphi(t_{i,N,1}), \ldots, \\ & \varphi(t_{i,1,M}), \ldots, \varphi(t_{i,N,M})]^{\mathrm{T}}. \end{aligned} \tag{8}$$

With this definition the output signal of the receive antenna array in the presence of phase noise can be expressed as

$$\mathbf{Y} = \left[\sum_{\ell=1}^{L} \mathbf{s}(\boldsymbol{\theta}_\ell)\right] \circ \mathbf{exp}(j\boldsymbol{\varphi}) + \mathbf{w}, \tag{9}$$

where $\circ$ denotes the Hadamard product. Approximating the term $\mathbf{exp}(j\boldsymbol{\varphi})$ in (10) by its 1st order Taylor expansion yields

$$\mathbf{Y} \approx \left[\sum_{\ell=1}^{L} \mathbf{s}(\boldsymbol{\theta}_\ell)\right] \circ [1 + j\boldsymbol{\varphi}] + \mathbf{w}. \tag{10}$$

## III. Parameter estimation using the SAGE algorithm

We resort to the SAGE algorithm as a low complexity method to approximate the maximum-likelihood estimates of the parameters $\boldsymbol{\theta}_\ell$, $\ell = 1, \ldots, L$ in (4). In the sequel we keep the same terminology as used in [1] and [2]. We select

$$\mathbf{X}_\ell = \mathbf{s}\left(\boldsymbol{\theta}_\ell\right) \circ \left[1 + j\boldsymbol{\varphi}\right] + \mathbf{w}'_\ell, \quad \ell = \mathrm{mod}(i, L) \tag{11}$$

as the hidden data in the $i$th iteration. Here, $\mathbf{w}'_\ell \in \mathbb{C}^{NM \times I}$ are independent matrix-valued complex white Gaussian noises with component variance $\sigma^2_{w'_\ell} = \beta_\ell \sigma^2_w$. The nonnegative parameters $\beta_\ell$, $\ell = 1, \ldots, L$ satisfy $\sum_{\ell=1}^{L} \beta_\ell = 1$. We assume that the phase noise covariance matrix $\mathbf{R}_{\boldsymbol{\varphi}} = E\left[\left(\boldsymbol{\varphi} - E\left[\boldsymbol{\varphi}\right]\right)\left(\boldsymbol{\varphi} - E\left[\boldsymbol{\varphi}\right]\right)^{\mathrm{T}}\right]$ and the noise variance $\sigma^2_w$ are known. The parameter subset associated with the hidden-data $\mathbf{X}_\ell$ in (11) is selected to be $\boldsymbol{\theta}_\ell$. It can be shown that the probability density functions $f\left(\mathbf{y}\,|\mathbf{x}_\ell\,, \boldsymbol{\theta}_\ell\right)$ and $f\left(\mathbf{x}_\ell | \boldsymbol{\theta}\right)$ are Gaussian with expectation $\sum\limits_{\ell' \neq \ell} \mathbf{s}\left(\boldsymbol{\theta}_{\ell'}\right)$ and $\mathbf{s}\left(\boldsymbol{\theta}_\ell\right)$ respectively and covariance matrices $\left[\sum\limits_{\ell' \neq \ell} \sum\limits_{\ell'' \neq \ell} \mathbf{s}\left(\boldsymbol{\theta}_{\ell'}\right) \mathbf{s}^{\mathrm{H}}\left(\boldsymbol{\theta}_{\ell''}\right)\right] \circ \mathbf{R}_{\boldsymbol{\varphi}} + \sigma^2_w \mathbf{I}$ and $\boldsymbol{\Sigma}_{\mathbf{X}_\ell}(\boldsymbol{\theta}_\ell) = \left[\mathbf{s}\left(\boldsymbol{\theta}_\ell\right) \mathbf{s}^{\mathrm{H}}\left(\boldsymbol{\theta}_\ell\right)\right] \circ \mathbf{R}_{\boldsymbol{\varphi}} + \sigma^2_{w'} \mathbf{I}$ respectively. Therefore, the selected hidden-data in (11) is admissible for the estimation of $\boldsymbol{\theta}_\ell$ in the sense defined in [1].

In the expectation (E-) step of the $i$th iteration, the so-called $Q$ function of $\boldsymbol{\theta}_\ell$ conditioned on the observation $\mathbf{Y} = \mathbf{y}$ and assuming a guess $\boldsymbol{\theta}^{[i-1]}$ for the parameter vector $\boldsymbol{\theta}$

$$\begin{aligned} Q\left(\boldsymbol{\theta}_\ell; \boldsymbol{\theta}^{[i-1]}\right) = \int \log f(\mathbf{x}_\ell | \boldsymbol{\theta}_\ell, \boldsymbol{\theta}^{[i-1]}_{\tilde{\ell}}) \cdot \\ f(\mathbf{x}_\ell\,|\mathbf{Y} = \mathbf{y};\, \boldsymbol{\theta}^{[i-1]}) d\mathbf{x}_\ell, \end{aligned} \tag{12}$$

is computed. In (12) $\boldsymbol{\theta}_{\tilde{\ell}}$ denotes the complement of $\boldsymbol{\theta}_\ell$ in $\boldsymbol{\theta}$ Inserting

$$\begin{aligned} f\left(\mathbf{x}_\ell; \boldsymbol{\theta}_\ell\right) = \frac{1}{(\pi)^N \left|\boldsymbol{\Sigma}_{\mathbf{X}_\ell}(\boldsymbol{\theta}_\ell)\right|} \cdot \\ \exp\left\{-\left(\mathbf{x}_\ell - \mathbf{s}\left(\boldsymbol{\theta}_\ell\right)\right)^{\mathrm{H}} \boldsymbol{\Sigma}^{-1}_{\mathbf{X}_\ell}\left(\boldsymbol{\theta}_\ell\right)\left(\mathbf{x}_\ell - \mathbf{s}\left(\boldsymbol{\theta}_\ell\right)\right)\right\}, \end{aligned} \tag{13}$$

in (12) yields after some straightforward algebraic manipulations

$$\begin{aligned} Q\left(\boldsymbol{\theta}_\ell; \boldsymbol{\theta}^{[i-1]}\right) = {} & A(\boldsymbol{\theta}_\ell) - \mathrm{tr}\{\boldsymbol{\Sigma}^{-1}_{\mathbf{X}_\ell}\left(\boldsymbol{\theta}_\ell\right)\left(\boldsymbol{\Sigma}_{\mathbf{X}_\ell}(\boldsymbol{\theta}^{[i-1]}_\ell)\right. \\ & - \boldsymbol{\Sigma}_{\mathbf{X}_\ell \mathbf{Y}}(\boldsymbol{\theta}^{[i-1]}_\ell) \boldsymbol{\Sigma}^{-1}_{\mathbf{YY}}(\boldsymbol{\theta}^{[i-1]}_\ell) \boldsymbol{\Sigma}^{\mathrm{H}}_{\mathbf{X}_\ell \mathbf{Y}}(\boldsymbol{\theta}^{[i-1]}_\ell) \\ & \left. + \boldsymbol{\mu}_{\mathbf{X}_\ell|\mathbf{Y}}\left(\boldsymbol{\theta}_\ell; \boldsymbol{\theta}^{[i-1]}_\ell\right) \boldsymbol{\mu}^{\mathrm{H}}_{\mathbf{X}_\ell|\mathbf{Y}}\left(\boldsymbol{\theta}^{[i-1]}_\ell\right)\right)\} \\ & + 2\Re\left\{\mathbf{s}^{\mathrm{H}}\left(\boldsymbol{\theta}_\ell\right) \boldsymbol{\Sigma}^{-1}_{\mathbf{X}_\ell}\left(\boldsymbol{\theta}_\ell\right) \boldsymbol{\mu}_{\mathbf{X}_\ell|\mathbf{Y}}\left(\boldsymbol{\theta}^{[i-1]}_\ell\right)\right\} \\ & - \mathbf{s}^{\mathrm{H}}\left(\boldsymbol{\theta}_\ell\right) \boldsymbol{\Sigma}^{-1}_{\mathbf{X}_\ell}(\boldsymbol{\theta}_\ell) \mathbf{s}\left(\boldsymbol{\theta}_\ell\right), \end{aligned} \tag{14}$$

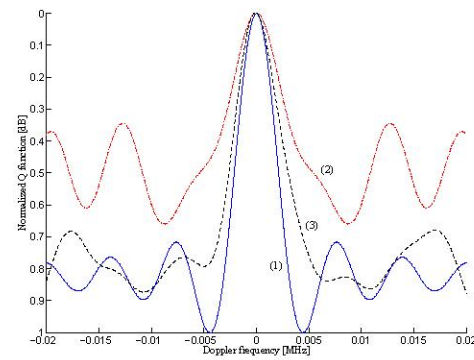


Fig. 3. Normalized $Q$-function (12) for the Doppler frequency of (1) the traditional SAGE algorithm without phase noise (continuous line), (2) the traditional SAGE algorithm with phase noise (dash-dot line), and (3) the new SAGE algorithm with phase noise (dash line).

where

$$\begin{aligned} A(\boldsymbol{\theta}_\ell) = {} & -\log\left((\pi)^N \left|\left[\mathbf{s}\left(\boldsymbol{\theta}_\ell\right) \mathbf{s}^{\mathrm{H}}\left(\boldsymbol{\theta}_\ell\right)\right] \circ \mathbf{R}_{\boldsymbol{\varphi}} \right.\right. \\ & \left.\left. + \sigma^2_{w'} \mathbf{I}\right|\right), \\ \boldsymbol{\mu}_{\mathbf{X}_\ell|\mathbf{Y}}\left(\boldsymbol{\theta}_\ell; \boldsymbol{\theta}^{[i-1]}_\ell\right) = {} & \mathbf{s}\left(\boldsymbol{\theta}_\ell\right) + \boldsymbol{\Sigma}_{\mathbf{X}_\ell \mathbf{Y}}(\boldsymbol{\theta}^{[i-1]}_\ell) \cdot \\ & \boldsymbol{\Sigma}^{-1}_{\mathbf{Y}}(\boldsymbol{\theta}^{[i-1]}_\ell)\left(\mathbf{y} - \sum_{\ell=1}^{L} \mathbf{s}(\boldsymbol{\theta}^{[i-1]}_\ell)\right), \end{aligned}$$

with

$$\begin{aligned} \boldsymbol{\Sigma}_{\mathbf{YY}}(\boldsymbol{\theta}^{[i-1]}_\ell) = {} & [\sum_{\ell=1}^{L} \mathbf{s}(\boldsymbol{\theta}^{[i-1]}_\ell) \mathbf{s}^{\mathrm{H}}(\boldsymbol{\theta}^{[i-1]})] \circ \mathbf{R}_{\boldsymbol{\varphi}} \\ & + \sigma^2_w \mathbf{I}, \\ \boldsymbol{\Sigma}_{\mathbf{X}_\ell \mathbf{Y}}(\boldsymbol{\theta}^{[i-1]}_\ell) = {} & [\mathbf{s}(\boldsymbol{\theta}^{[i-1]}_\ell) \sum_{\ell=1}^{L} \mathbf{s}(\boldsymbol{\theta}^{[i-1]}_\ell)^{\mathrm{H}}] \circ \mathbf{R}_{\boldsymbol{\varphi}} \\ & + E[\mathbf{w}' \mathbf{w}^{\mathrm{H}}]. \end{aligned} \tag{15}$$

Note that $Q(\boldsymbol{\theta}_\ell; \boldsymbol{\theta}^{[i-1]})$ in (14) reduces to the form derived in [1] when $\mathbf{R}_{\boldsymbol{\varphi}} = \mathbf{0}$. In the Maximization (M-) step of the $i^{\mathrm{th}}$ iteration, the estimate ${\boldsymbol{\theta}_\ell}^{[i]}$ of $\boldsymbol{\theta}_\ell$ is computed to be

$$\boldsymbol{\theta}^{[i]}_\ell = \arg\max_{\boldsymbol{\theta}_\ell} \left\{Q\left(\boldsymbol{\theta}_\ell; \boldsymbol{\theta}^{[i-1]}\right)\right\}. \tag{16}$$

The maximization operation in (16) is simplified by splitting the joint optimization with respect to $\boldsymbol{\theta}_\ell$ in separate one-dimensional coordinate-wise optimizations as described in [2].

## IV. Performance Evaluation in Synthetic Channels

We investigate the performance of the proposed SAGE algorithm for the narrowband case, i.e. where the propagation delay cannot be resolved. A one-path scenario and a two-path scenario with horizontal-only propagation are considered in this study. The weights of the paths in terms of SNR per path are assumed to be large enough (40 dB) so that the effect of additive noise can be neglected. The path parameters

TABLE I
PROPAGATION SCENARIO CONSIDERED FOR THE MONTE CARLO SIMULATIONS.

| Path Parameters | One-Path Scenario | Two-Path Scenario | |
|---|---|---|---|
| | | Path 1 | Path 2 |
| SNR [dB] | 40 | 40 | 40 |
| Doppler frequency [Hz] | 0 | 0 | 0 |
| Co-elevation of departure [radian] | $\pi/2$ | $\pi/2$ | $\pi/2$ |
| Co-elevation of arrival [radian] | $\pi/2$ | $\pi/2$ | $\pi/2$ |
| Azimuth of departure [radian] | $\pi/2$ | $\pi/2$ | $\pi/4$ |
| Azimuth of arrival [radian] | $\pi/2$ | $\pi/2$ | $\pi/4$ |

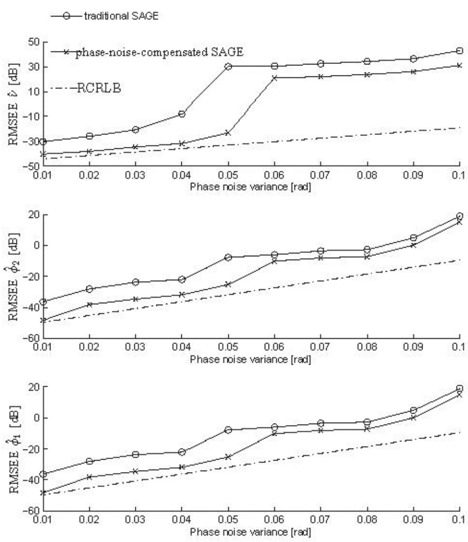


Fig. 4. RMSEEs and RCLRBs for the Doppler frequency, the azimuth of departure, and the azimuth of arrival versus the phase noise variance in the one-path scenario.

characterizing these scenarios are reported in Table I. We assume that the transmit and receive arrays are uniform and linear with $M = N = 8$ half-a-wavelength spaced elements. The sounding sequence has period $L = 127$ and chip duration $T_c = 10ns$. The correlation matrix $\mathbf{R}_{\varphi}$ is computed from the short-term correlation function of phase noise reported in [4]. The Doppler frequency, the azimuth of departure and the azimuth of arrival are jointly estimated with the proposed method, while the co-elevations of the paths are assumed to be known.

First we present the results obtained in the one-path scenario. Fig. 3 depicts the $Q$-functions of the Doppler frequency for (1) the traditional SAGE algorithm [2] without phase noise, (2) the traditional SAGE algorithm with phase noise, and (3) the new SAGE algorithm with phase noise. It can be observed that the $Q$-function in the case (2) has higher side-lobes and a wider main-lobe than the $Q$-function in case (1). The width of the main-lobe and the height of the sidelobes of the $Q$-functions in case (3) are lower compared to those of the $Q$-function in case (2). This observation explains why the new SAGE algorithm outperforms the tradition SAGE algorithm in the presence of phase noise, as the next results will show.

The root mean-square estimation errors (RMSEEs) of the parameter estimates returned by the traditional SAGE algorithm and the new proposed SAGE algorithm have been assessed by means of Monte Carlo simulations in the presence of phase noise. They are reported with the their respective root CRLBs (RCRLBs) versus the phase noise variance in Fig. 4. It can be observed that the RMSEEs increase with the variance and that the new proposed SAGE algorithm outperforms the traditional SAGE algorithm in terms of lower RMSEEs. When the phase noise variance is below a certain threshold, i.e. 0.05 radian, the RMSEEs achieved with the new proposed SAGE algorithm are close to their corresponding RCRLBs derived in the one-path scenario. In this range the RMSEEs obtained with the new proposed SAGE algorithm are lower by about 10 dB compared to the corresponding RMSEEs achieved with the traditional SAGE algorithm. Above this threshold the performance of the estimators significantly deteriorates.

The RMSEEs for the parameters of the two paths in the two-path scenario are reported in Fig. 5 (Path 1) and Fig. 6 (Path 2). We observe a slight degradation compared to the results obtained for the one-path scenario. However, the RMSEEs curves for both paths behave similarly to their counterpart in the one-path scenario. In particular the new proposed SAGE algorithm always outperforms the traditional SAGE algorithm and the same threshold effect can be observed below which the effect of phase noise can be almost mitigated.

Actual measured phase noise variances of the local oscillators at the transmitter and the receiver of channel sounders lie in the range 0.02 to 0.03 radian [4], i.e. below the above threshold. In this case, i.e. for the considered sounding sequence, the new SAGE algorithm is able to compensate for the effect of phase noise. More generally, the new scheme is able to compensate for the effect of phase noise, provided the used sounding sequence is short enough. Indeed, as we can see in (14) and (15), the length of the sounding sequence affects the performance of the new algorithm via the correlation matrix $\mathbf{R}_{\varphi}$. Further investigations are necessary to quantify the relationship between the maximum duration of the sounding sequence and the short-term statistics of phase noise for the new SAGE algorithm to be able to operate close to the CRLBs for the path parameters.

## V. CONCLUSIONS

In this contribution, we proposed a new version of the SAGE algorithm for path parameter estimation which compensates

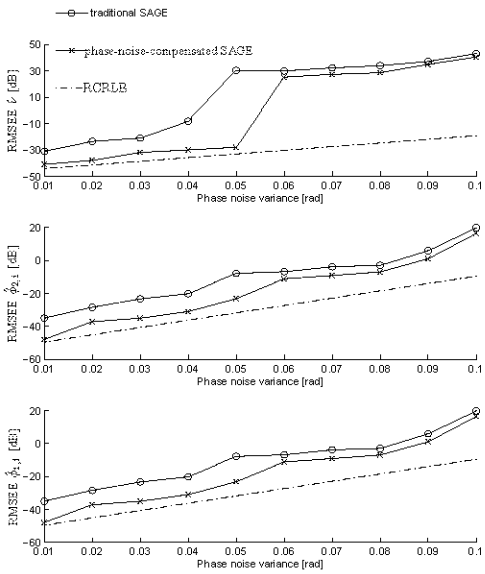


Fig. 5. RMSEEs and RCLRBs for the Doppler frequency, the azimuth of departure, and the azimuth of arrival of the first path versus the phase noise variance in the two-path scenario.

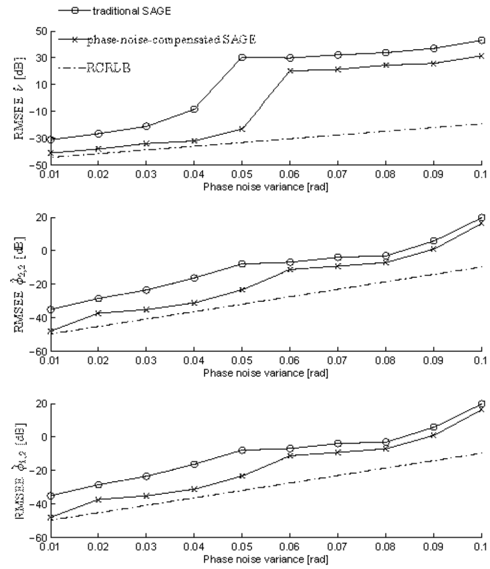


Fig. 6. RMSEEs and RCLRBs for the Doppler frequency, the azimuth of departure, and the azimuth of arrival of the second path versus the phase noise variance in the two-path scenario.

for the effect of phase noise. The new algorithm reduces to the traditional SAGE algorithm derived in [2], when the phase noise covariance matrix vanishes.

We first contrasted the two algorithms in a narrowband one-path scenario. The $Q$-functions derived in the E-steps of the algorithms for the Doppler frequency were compared. The $Q$-function obtained with the new SAGE algorithm exhibits a narrower main lobe and lower side-lobes than those of the $Q$-function computed using the traditional SAGE algorithm in the presence of phase noise. This behaviour explains the better behaviour of the former algorithm observed in terms of improved root mean-square estimation errors (RMSEEs) for the path parameter estimates. The RMSEES for the path parameters were assessed my means of Monte Carlo simulations in the one-path scenario and in a two-path scenario. The results show that the new SAGE algorithm always outperforms the traditional algorithm in terms of lower RMSEEs. Moreover, provided the phase noise variance is below a certain threshold, the RMSEEs are close to the root Cramér-Rao lower bounds. The results show that for sufficient short sounding sequences the new SAGE algorithm is able to compensate for the effect of phase noise in practical channel sounding equipments. Further investigations are needed to quantitatively assess the relationship between the maximum length of the used sounding sequence and the short-term statistics of phase noise for the new scheme to be able to operate close to the CRLBs for the path parameters.

## Acknowledgment

This research was supported by the National Technology Agency of Finland (TEKES), Nokia, the Finnish Defence Forces and Elektrobit through the PANU-project. It was also supported by the FP6 Network of Excellence in Wireless Communications (NEWCOM). The authors also would like to thank Troels Pedersen for his very valuable comments.

## References

[1] J. A. Fessler and A. O. Hero, "Space-alternating generalized expectation-maximization algorithm," *IEEE Trans. Signal Processing*, vol. 42, pp. 2664-2677, Oct. 1994.

[2] B. H. Fleury, P. Jourdan, and A. Stucki, "High-resolution channel parameter estimation for MIMO applications using the SAGE algorithm," *Int. Zurich Seminar*, Feb. 2002.

[3] X. Yin, B. H. Fleury, P. Jourdan, and A. Stucki, "Polarization Estimation of Individual Propagation Paths Using the SAGE Algorithm," *IEEE International Symposium on Personal, Indoor and Mobile Radio Communications*, Sep. 2003.

[4] D. S. Baum and H. Bölcskei, "Impact of phase noise on MIMO channel measurement accuracy," *IEEE Vehicular Technology Conference*, Sep. 2004.

[5] A. Taparugssanagorn, J. Ylitalo, B. H. Fleury, "Phase-Noise in TDM-switched MIMO Channel Sounding and Its Impact on Channel Capacity Estimation," *IEEE Global Telecommunications*, Nov. 2007.

[6] P. Almers, S. Wyne, F. Tufvesson, and A. F. Molisch, "Effect of Random Walk Phase Noise on MIMO Measurements," *IEEE Vehicular technology Conference*, Stockholm, May 30-June 2005.

[7] A. Taparugssanagorn, M. Alatossava, V.-M. Holappa and J. Ylitalo, "Impact of Channel Sounder Phase Noise on Directional Channel Estimation by SAGE," *IET Microwaves, Antennas & Propagation*, vol. 1, Issue 3, pp. 803-808, June 2007.

[8] B. H. Fleury, P. Jourdan, and A. Stucki, "High-resolution channel parameter estimation for MIMO applications using the SAGE algorithm," *Int. Zurich Seminar BroadBand Communications. Access, Transmission, Networking*, pp. 30-130-9, Feb. 2002.

[9] T. Pedersen, C. Pedersen, X. Yin, B. Fleury, R. Pedersen, B. Bozinovska, A. Hviid, P. Jourdan, and A. Stucki, "Joint Estimation of Doppler Frequency and Directions in Channel Sounding Using Switched Tx and Rx Arrays," *IEEE Global Telecommunications*, pp. 2354-2360, Dec. 2004.